

DOI:10.16781/j.0258-879x.2016.01.0010

· 论著 ·

## 兔胰腺移植瘤纳米刀、冷冻、射频的对比研究

宁周雨<sup>1</sup>,王鹏<sup>1</sup>,陈颢<sup>1</sup>,解婧<sup>1</sup>,林钧华<sup>1</sup>,朱晓燕<sup>1</sup>,陈其文<sup>1</sup>,徐立涛<sup>1</sup>,宋利斌<sup>1</sup>,高嵩<sup>1</sup>,姜峰<sup>2</sup>,孟志强<sup>1\*</sup>

1. 复旦大学附属肿瘤医院中西医结合科,上海 200032

2. 潍坊诸城中医医院肿瘤科,潍坊 262200

**[摘要]** **目的** 通过研究胰腺移植瘤不可逆电穿孔(irreversible electroporation, IRE, 俗称“纳米刀”)、冷冻、射频术后的肿瘤凋亡、机体免疫反应及血管生成因子情况,观察不同微创技术对胰腺移植瘤的抗肿瘤效果。**方法** 兔胰腺移植瘤模型8只,并随机分为模型对照组、纳米刀治疗组、冷冻治疗组及射频治疗组,每组2只。动态观察治疗过程中新西兰大白兔的生命体征,于治疗后第1天全部处死,分离血浆及血清进行检测,H-E染色观察移植瘤组织形态学改变,免疫组织化学方法检测Bcl-2、HSP70和VEGF在胰腺癌移植瘤中的表达,Tunnel法检测细胞凋亡。**结果** 各组实验兔术后均存活。肉眼观肿瘤边界清晰,触之质地较硬,各组治疗区域可见明显凝固性坏死改变。H-E染色显示治疗组坏死区域和正常区域边界清晰,以纳米刀组为著。各组坏死边缘区可见大量红细胞以及炎症细胞浸润,冷冻及射频术区仍可见部分存活细胞。Tunnel结果显示,射频治疗可以明显增加胰腺癌细胞凋亡。与模型对照组相比,各治疗组血浆的Caspase-3、TNF- $\alpha$ 及VEGF水平升高;术区Bcl-2及VEGF因子表达降低,HSP70表达升高。术后血清学检测结果显示仅纳米刀治疗后新西兰大白兔的肌酸激酶水平升高,冷冻及射频组未见升高;肌钙蛋白、肝肾功能及血清淀粉酶未见异常。**结论** 纳米刀、冷冻、射频治疗兔胰腺移植瘤时,均可能通过诱导细胞凋亡、产生特异的抗肿瘤免疫效应及抑制血管生成来抑制兔胰腺移植瘤的生长,且治疗方法安全、有效。纳米刀在激发机体肿瘤免疫和保护周围重要脏器上有一定的优势。

**[关键词]** 胰腺肿瘤;异种移植;纳米刀;冷冻消融;射频消融;细胞凋亡;肿瘤免疫;安全性

**[中图分类号]** R 735.9      **[文献标志码]** A      **[文章编号]** 0258-879X(2016)01-0010-07

## A comparative study of nanoknife, cryoablation, and radiofrequency ablation for treatment of pancreatic cancer xenograft in rabbits

NING Zhou-yu<sup>1</sup>, WANG Peng<sup>1</sup>, CHEN Hao<sup>1</sup>, XIE Jing<sup>1</sup>, LIN Jun-hua<sup>1</sup>, ZHU Xiao-yan<sup>1</sup>, CHEN Qi-wen<sup>1</sup>, XU Li-tao<sup>1</sup>, SONG Li-bin<sup>1</sup>, GAO Song<sup>1</sup>, JIANG Feng<sup>2</sup>, MENG Zhi-qiang<sup>1\*</sup>

1. Department of Integrative Cancer, Fudan University Shanghai Cancer Center, Shanghai 200032, China

2. Department of Oncology, Weifang Zhucheng Traditional Chinese Medicine Hospital, Weifang 262200, Shandong, China

**[Abstract]** **Objective** To investigate the apoptosis, immunity response and angiogenesis factor changes in rabbits with pancreatic cancer xenografts after treatment with irreversible electroporation (IRE, commonly known as nanoknife), cryoablation, or radiofrequency ablation (RFA), and to observe the antitumor effects of the above minimally invasive techniques for pancreatic cancer xenografts. **Methods** Eight pancreatic cancer xenograft model rabbits were randomly divided into the control, IRE, cryoablation, and RFA groups, with each group containing 2 rabbits. The vital signs of the animals were observed during the treatment and all the rabbits were executed on the next day after treatment. The serum samples were collected to examine the liver, kidney function and creatine kinase levels; and ELISA method was used to detect the cardiac troponin I(CTnI), Caspase-3, tumor necrosis factor- $\alpha$  (TNF- $\alpha$ ) and vascular endothelial growth factor(VEGF) levels in the plasma. Morphological changes of the tumor tissues were subjected to H-E staining, and Tunnel assay was used to detect the apoptosis of tumor cells. Immunohistochemistry method was applied to detect Bcl-2, HSP70 and VEGF expression in pancreatic cancer xenograft tissues. **Results** All the rabbits survived after treatment. The tumors had a clear border and were hard in texture. Obvious coagulative necrosis areas were seen in the treatment areas in each treatment group. H-E staining showed a clear borderline between the necrotic and normal areas, which was especially true in the IRE group. A large number of red blood cells and inflammatory cell infiltration were seen around the border of the necrosis in each group, with some live cells seen in the

[收稿日期] 2015-10-23      [接受日期] 2016-01-03

[作者简介] 宁周雨,博士生. E-mail: yuzhou3065@126.com

\* 通信作者(Corresponding author). Tel: 021-64175590-83629, E-mail: mengzhq@yeah.net

cryoablation and RFA groups. Tunnel assay showed that RFA significantly increased the apoptosis in pancreatic cancer cells compared with the other two treatment groups. The plasma Caspase-3, TNF- $\alpha$  and VEGF levels were increased in each treatment group. Bcl-2 and VEGF expression was decreased and HSP70 expression was increased in the treatment areas. Post-treatment serological test showed that serum amylase, liver, kidney functions and CTnI were all within the normal range, except for a significantly higher level of creatine kinase in the IRE group. **Conclusion** IRE, cryoablation, and RFA can inhibit pancreatic cancer xenograft through inducing apoptosis, producing specific antitumor immune response and inhibiting angiogenesis; they are safe and effective. IRE has certain advantages in producing specific antitumor immune response and protecting important peripheral organs.

**[Key words]** pancreatic neoplasms; xenografts; nano knife; cryoablation; radiofrequency ablation; apoptosis; tumor immunity; security

[Acad J Sec Mil Med Univ, 2016, 37(1): 10-16]

胰腺癌是常见的消化系统肿瘤之一,占世界恶性肿瘤发病率的第10位(3%),而死亡率为第4位(7%),发病率及死亡率在人群中均呈上升趋势<sup>[1]</sup>。胰腺癌起病隐匿,早期诊断率低,恶性程度高,手术切除率低,对放疗、化疗不敏感,临床预后极差,5年生存率低于6%,为唯一发病率与病死率相当的恶性肿瘤<sup>[1]</sup>。局部进展期及转移性胰腺癌约占全部胰腺癌的80%,局部晚期中位生存期为6~10个月,转移性胰腺癌中位生存期仅3~6个月<sup>[1]</sup>。对于局部晚期和转移性胰腺癌,局部消融治疗可达到消灭肿瘤、减轻疼痛、延长患者生存期的目的。目前国内常见的消融治疗主要有射频消融(radiofrequency ablation, RFA)、微波消融(microwave ablation, MWA)、冷冻消融(cryoablation)和高强度聚焦超声(high-intensity focused ultrasound, HIFU),且被证实可延长局部晚期及转移性胰腺癌患者生存期,但是受到适应证、禁忌证和不良反应等因素的限制,治疗效果仍不理想。不可逆电穿孔(irreversible electroporation, IRE, 俗称“纳米刀”)治疗肿瘤是通过释放kV级高压的直流电,以电脉冲方式产生强力的电场,在细胞膜上产生永久性的纳米孔,促进肿瘤细胞凋亡,消融肿瘤组织。本研究选取新西兰大白兔VX2胰腺移植瘤为研究对象,探究纳米刀、冷冻和射频消融除直接消融肿瘤组织外的其他抗肿瘤机制,同时探讨纳米刀在治疗胰腺移植瘤的安全性和有效性。

## 1 材料和方法

1.1 新西兰大白兔VX2胰腺移植肿瘤模型建立 新西兰大白兔8只,体质量为2.1~3.4 kg,购自上海斯莱克实验动物中心〔动物生产许可证号:SCXK(沪)2014-0008〕。氯胺酮4~6 mg/kg肌肉注

射麻醉新西兰大白兔,左上腹部中线旁行1 cm的纵行切口,将1 mm<sup>3</sup>瘤块植入胰体尾处,术后3 d内常规肌肉注射抗生素,生长2周后可见直径约2 cm肿瘤结节(图1A)。

1.2 实验分组及手术实施 将实验兔分为模型对照组、纳米刀组、冷冻组、射频组,每组2只。纳米刀治疗过程中全麻配合气管插管(氯胺酮0.1~0.15 mg/只,配合肌松药氯化琥珀胆碱0.1~0.2 mg/只),术后简易呼吸器复苏,余治疗组以氯胺酮0.1~0.15 mg/只麻醉,麻醉满意后开腹暴露胰腺移植瘤,将电极插入肿瘤组织内。纳米刀实验参数:AngioDynamics公司制造的纳米刀正负两电极,正负电极之间的距离为1.0~1.5 cm,进针深度为1.0~1.5 cm,电压1 800~2 400 V/cm,脉冲长度70/s,脉冲数目10,脉冲时值90  $\mu$ s(图1B)。冷冻参数:采用美国氩氦刀冷冻系统进行治疗,冷冻探针为1.47 mm,冷冻消融肿瘤模式为:氩气急剧降温冷冻5 min,氦气快速复温2 min为1个循环,共2个冷冻/复温循环(图1C)。射频参数:采用RF-2000射频消融仪及MEDSPHERE电外科电极,将MEDSPHERE电外科电极针准确插入病灶内,射频输出功率150 W,治疗总时间为8~13 min(图1D)。

1.3 样本处理及检测 所有实验兔术后24 h处死,取血,分析血清和血浆,各组标本经甲醛固定处理。血清进行肝肾功能、淀粉酶(AMY)、肌酸激酶检查,血浆标本采用酶标仪双抗体夹心(ELISA)法测定心肌肌钙蛋白I(CTnI)、Caspase-3、肿瘤坏死因子(TNF)- $\alpha$ 及血管内皮生长因子(vascular endothelial growth factor, VEGF)的生物学活性。H-E染色后光镜下观察各组术后移植瘤组织的形态学改变,同时Tunnel试剂染色,共聚焦显微镜下拍照。采用

Envision法进行Bcl-2、VEGF、HSP70免疫组化染色,所用的一抗为:兔抗兔多克隆抗体Bcl-2(工作浓度为1:1 000,台湾Abnova公司,货号:PAB19562);鼠抗兔HSP70单克隆抗体(工作浓度为1:1 000,美国Abcam公司,货号:ab2787)、鼠抗兔VEGF多克隆抗体(工作浓度为1:1 000,美国Abcam公司,货号:ab1316)。HSP70、Bcl-2及VEGF染色阳性信号均呈棕黄色颗粒,HSP70、VEGF表达定位于细胞质,Bcl-2表达定位于细胞核及细胞质。

**1.4 统计学处理** 采用Graphpad prim 5和Excel软件进行图形绘制,Adobe Photoshop软件进行图形编辑。采用SPSS 19.0软件进行数据分析,两组数据间比较采用t检验,检验水准( $\alpha$ )为0.05。

## 2 结 果

**2.1 术后大体标本及组织病理学观察** 对照组实验兔脾胃间隙间可见直径约2 cm结节,肿瘤表面呈灰红色,质偏软,表面可见丰富的供瘤血管(图

1A);镜下见癌细胞密集,间质少,核大染色深,其大小和形态各异,染色浓淡不均,异常分裂像多见,细胞呈不规则排列,新生毛细血管丰富,肿瘤中心可见出血坏死(图1E)。

纳米刀组消融区边界清晰,核固缩、碎裂,蓝染;肿瘤血管变性坏死、血栓形成,内见红细胞碎裂物沉积,但血管腔结构完整(图1F)。

冷冻组肿瘤组织充血水肿,无光泽,触之较硬;镜下见细胞完全坏死崩解、核碎裂,呈凝固性坏死,坏死区域周边(冰球边缘)出现明显的损伤区带,其中仍可见部分癌细胞,但细胞皱缩,核浓集,染色质固缩,呈典型的凋亡细胞特征(图1G)。

射频组消融区中央完全坏死,见大片无定结构的粉染区,其周边为凝固性坏死;镜下见细胞核固缩、碎裂和溶解,内仍可见部分存活肿瘤细胞(图1H),术区边缘血管充血,可见大量凋亡细胞(图1I)。

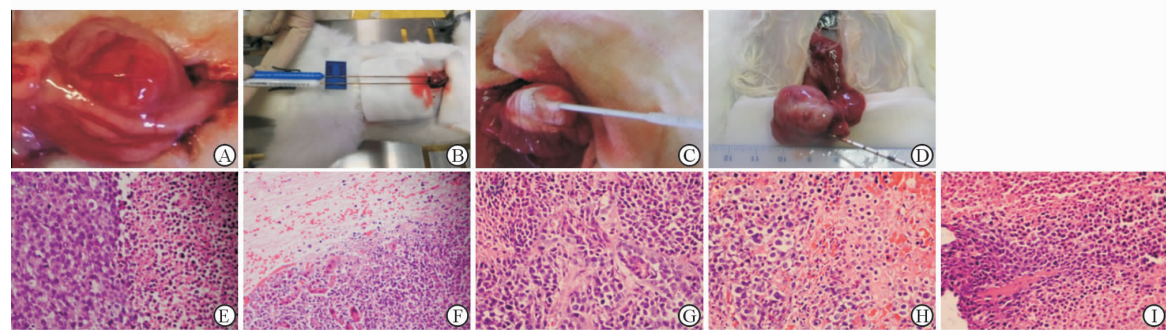


图1 各组实验兔胰腺移植瘤大体(A-D)及组织病理学(E-I)结果

**Fig 1 Gross specimen (A-D) and histopathological results (E-I) of pancreatic cancer xenografts in rabbits of each group**

A: Gross specimen of the rabbit pancreatic xenograft, with rich angiogenesis visible on the surface of tumor and adhered to the surrounding tissue; B-D: The schematic illustrations of irreversible electroporation (IRE), cryoablation, and radiofrequency ablation (RFA) treatment of rabbit pancreatic xenografts; E: In the control group, tumor cells were arranged closely, with markedly varied morphology, hemorrhage and necrosis; F: After IRE, tumor cell nuclei were compressed, and fragmentized or dissolved; G: Ablation area boundary was irregular, and some survival cells could be seen in the ablation area; H: Clear border was seen between the treatment area and the untreated area in the RFA group, with the necrosis area filled with red dye fragments; I: A large number of apoptotic cells could be seen in the RFA area. Original magnification:  $\times 400$  (E-I)

**2.2 肿瘤凋亡相关因子变化** Bcl-2家族是重要的凋亡相关因子,激活线粒体及内质网的内外凋亡通路发挥促肿瘤组织凋亡,Bax(促凋亡蛋白)/Bcl-2(促生存蛋白)的比值升高,促进Caspase-3表达,细胞接受凋亡信号刺激发生不可逆性凋亡。本实验血浆ELISA结果显示,各治疗组术后

机体Caspase-3水平均较对照组不同程度升高( $P < 0.01$ ,图2A)。Bcl-2主要表达于胞质,部分可见胞核浓染(图2B);与对照组比较,纳米刀治疗组及射频治疗组Bcl-2表达差异无统计学意义,而冷冻治疗组Bcl-2表达低于对照组( $P < 0.01$ ,图2C)。

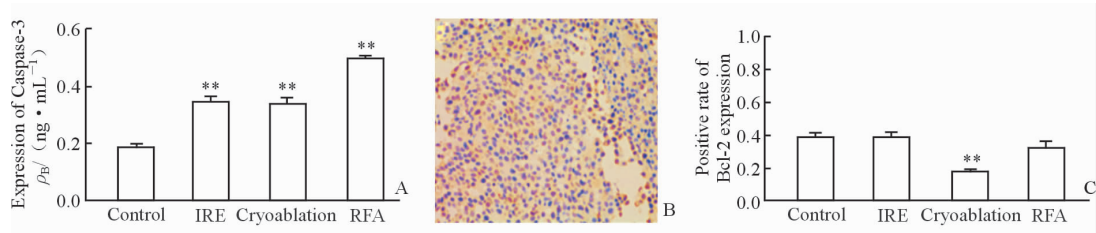


图 2 各组间肿瘤凋亡相关因子 Caspase-3、Bcl-2 的表达

Fig 2 Tumor apoptosis related factor Caspase-3 and Bcl-2 expression in the each group

A: Plasma Caspase-3 levels in each group; B: Bcl-2 expression in border of irreversible electroporation (IRE) treatment area; yellow dye could be seen in the cell cytoplasm and cell nucleus (Envision method, original magnification:  $\times 200$ ); C: Positive rate of Bcl-2 expression in each group. RFA: Radiofrequency ablation. \*\*  $P < 0.01$  vs control group.  $n=6$ ,  $\bar{x} \pm s$

Tunnel 方法又称 DNA 断裂的原位末端标记法,是用来检测组织细胞在凋亡早期过程中细胞核 DNA 的断裂情况,特异准确地定位正在凋亡的细胞。本实验各组消融区边缘肿瘤细胞可见典型 Tunnel 阳性细胞,有的散在分布见,有的集中分布(图 3),其中射频治疗组凋亡率最高(图 3D)。

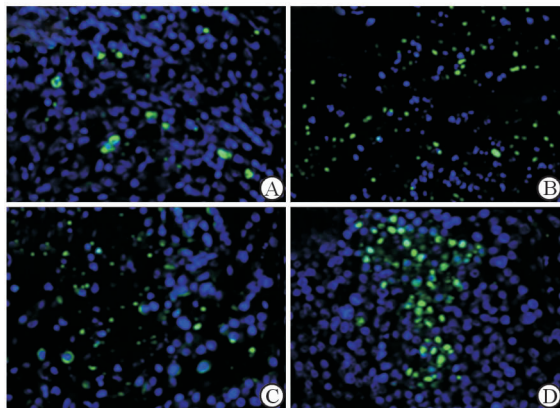


图 3 各组消融区边缘细胞凋亡情况

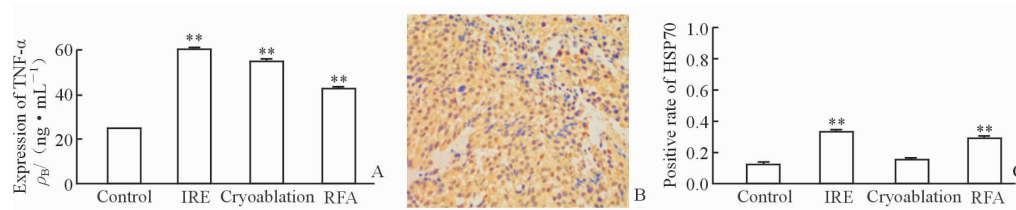
Fig 3 Apoptosis in ablation marginal cells after treatment in each group

A: Control group; B: Irreversible electroporation group; C: Cryoablation group; D: Radiofrequency ablation group. Original magnification:  $\times 200$

2.3 机体免疫因子生成情况 TNF- $\alpha$  是多效的促炎细胞因子,介导机体免疫调节功能。HSP70 是热休克蛋白家族中最保守、最重要的一族,在肿瘤免疫中发挥重要作用。各治疗组血浆 TNF- $\alpha$  水平及术区边缘(除冰冻治疗组) HSP70 表达量均较模型对照组升高( $P < 0.01$ ),尤以纳米刀治疗组最明显(图 4)。

2.4 肿瘤侵袭相关因子变化 VEGF 是一种功能最强的促血管生成因子,与肿瘤的侵袭、转移等生物学特性密切相关。各治疗组血浆 VEGF 水平均有所升高,以射频治疗组为著。术区 VEGF 淡染,以肿瘤边缘为主,冷冻治疗组 VEGF 下降最为明显,纳米刀治疗组及射频治疗组未见明显降低(图 5)。

2.5 各治疗技术的安全性 纳米刀治疗过程中实验兔伴随脉冲作用出现脉冲式肌肉强直收缩,射频及冷冻消融组治疗时未见异常。由表 1 可见,纳米刀治疗组实验兔出现肌酸激酶升高,冷冻治疗组及射频治疗组出现谷草转氨酶(AST)轻度升高;不同术式术后血清 AMY 均出现不同程度升高;肝肾功能未见明显异常。

图 4 各组血浆 TNF- $\alpha$  和术区边缘 HSP70 的表达水平Fig 4 Expression of plasma TNF- $\alpha$  and HSP70 in the border of treatment area in each group

A: Variation of plasma TNF- $\alpha$  level in each group; B: HSP70 expression in the border of irreversible electroporation (IRE) treatment area, with yellow dye seen in the cell cytoplasm and nucleus (Envision method, original magnification:  $\times 200$ ); C: The positive rate of HSP70 expression in each group. RFA: Radiofrequency ablation. \*\*  $P < 0.01$  vs control group.  $n=6$ ,  $\bar{x} \pm s$

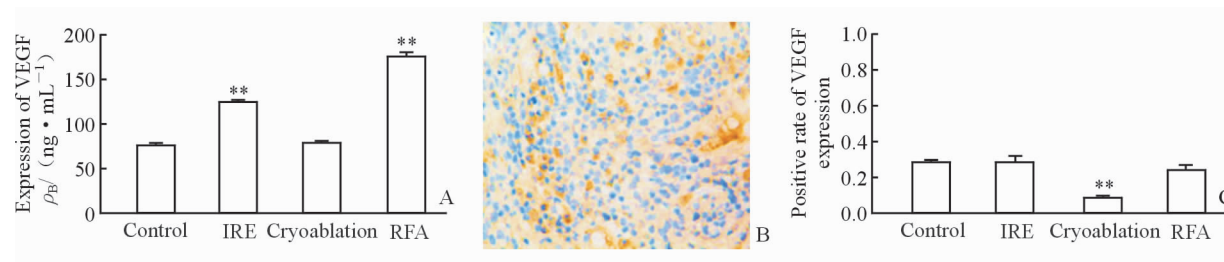


图 5 各组实验兔术后血浆及术区 VEGF 的表达水平

Fig 5 Post-treatment plasma and treatment area VEGF expression levels in rabbits of each group

A: Variation of plasma VEGF level in rabbits; B: VEGF expression in the edge of IRE treatment area, with yellow dye seen in the cell nucleus and partial cell cytoplasm (Envision method, original magnification:  $\times 200$ ); C: The positive rate of VEGF expression in each group. IRE: Irreversible electroporation; RFA: Radiofrequency ablation; VEGF: Vascular endothelial growth factor. \*\*  $P < 0.01$  vs control.  $n=6$ ,  $\bar{x} \pm s$

表 1 各组肝肾功能、淀粉酶、肌酸激酶及肌钙蛋白 I 变化

Tab 1 Variations of postoperative liver and kidney function, AMY, CK-MB and CTnI levels in each group

Group	ALB $\rho_B$ ( $\text{g} \cdot \text{L}^{-1}$ )	AST $\varepsilon_B$ ( $\text{U} \cdot \text{L}^{-1}$ )	GGT $\varepsilon_B$ ( $\text{U} \cdot \text{L}^{-1}$ )	ALT $\varepsilon_B$ ( $\text{U} \cdot \text{L}^{-1}$ )	ALP $\varepsilon_B$ ( $\text{U} \cdot \text{L}^{-1}$ )
Control	29	23	3	22	122
IRE	23	15	6	20	56
Cryoablation	22	81	2	21	35
RFA	20	50	6	18	42
Group	BUN $c_B$ ( $\text{mmol} \cdot \text{L}^{-1}$ )	CREA $c_B$ ( $\text{mmol} \cdot \text{L}^{-1}$ )	AMY $c_B$ ( $\text{mmol} \cdot \text{L}^{-1}$ )	CK-MB $\varepsilon_B$ ( $\text{U} \cdot \text{L}^{-1}$ )	CTnI $\rho_B$ ( $\text{ng} \cdot \text{mL}^{-1}$ )
Control	10.38	179.7	218	736	0.85
IRE	0.33	78.9	447	3 560	1.05
Cryoablation	84.7	184.7	250	655	1.92
RFA	30.4	130.4	284	575	2.17

IRE: Irreversible electroporation; RFA: Radiofrequency ablation; ALB: Albumin; AST: Aspartate aminotransferase; GGT: Gamma glutamyl transpeptidase; ALT: Alanine transaminase; ALP: Alkaline phosphatase; BUN: Blood urea nitrogen; CREA: Serum creatinine and urea nitrogen; AMY: Serum amylase; CK-MB: Creatine kinase-MB; CTnI: Cardiac troponin I

### 3 讨 论

目前晚期胰腺癌主要治疗手段仍是化疗,各种化疗方案对胰腺癌患者的总体生存期未见明显改善<sup>[2-4]</sup>,包括吉西他滨联合卡培他滨(中位生存期为7.1个月)、FOLFIRINOX(中位生存期为11.1个月)及白蛋白紫杉醇联合吉西他滨(总体生存期为8.5个月),所以胰腺癌治疗仍面临巨大挑战。积极寻找其他替代治疗方式及方案对改善胰腺癌患者生存期和生活质量具有重要的意义。既往晚期胰腺肿瘤局部冷冻、射频作为一种姑息性治疗方式取得一定的理想效果,但是由于临近腹腔大血管及胆道系统,存在出血、胆漏及胰漏风险,而且其具体参数的设置及操作要点尚需更进一步的研究和探讨<sup>[5-7]</sup>。纳米刀作为非热效应的一种新兴微创治疗手段,大大减少了胰腺癌治疗导致的消化道出血及胆道损

伤,发展前景广阔<sup>[8-10]</sup>。本研究通过抗肿瘤的安全性和有效性探讨纳米刀在治疗不可切除性胰腺癌的优势。

本实验结果发现,纳米刀治疗组的血管结构未见明显破坏,内可见多量破碎红细胞沉积;纳米刀灭活区域和非灭活区域之间存在明显分界线,而冷冻或射频等其他热灭活方法则产生一片无定形区域,这片区域很有可能存在不完全灭活的组织而造成部分肿瘤细胞残余或肿瘤复发<sup>[11]</sup>。这一结果与纳米刀破坏细胞膜的完整性、继而发生细胞凋亡或坏死、但不影响由蛋白质为主要构成成分的组织框架结构<sup>[12]</sup>有关,纳米刀有可能成为治疗毗邻神经、血管等重要敏感组织肿瘤(晚期胰腺癌、邻近门静脉及胆道的肝恶性肿瘤结节)的一种有效方法。

纳米刀、冷冻及射频消融除能直接毁损肿瘤组织外,还均能通过促肿瘤组织凋亡、增强机体免疫及

抑制肿瘤侵袭转移等机制发挥抗肿瘤作用,但存在细微的差别,这与三者的消融机制不同有关:纳米刀通过一定的电脉冲剂量使细胞膜出现不可恢复的破裂,导致细胞死亡<sup>[13]</sup>;冷冻消融是先通过冷冻使癌细胞内形成冰晶,再快速升温使细胞内的冰晶爆裂,癌细胞被完全摧毁,通过这种快速制冷和急速升温来抗肿瘤<sup>[14]</sup>。射频消融通过一定的射频输出,使靶区组织细胞离子振荡摩擦产生热量,局部温度可达80℃~90℃,足以使肿瘤组织产生凝固性坏死,并最终形成液化灶或纤维组织,达到治疗肿瘤目的<sup>[15]</sup>。

Bcl-2是Bcl-2家族重要的促生存蛋白因子,Bcl-2的降低促发肿瘤凋亡<sup>[16]</sup>,同时促进Caspase-3这一重要促凋亡因子的表达,进而导致肿瘤细胞发生不可逆性凋亡<sup>[17]</sup>。本实验血浆ELISA结果显示,与对照组比较,各治疗组Caspase-3水平不同程度升高,射频治疗组消融范围较其余治疗组显著,而冷冻治疗组的Bcl-2下降最为明显,与消融区Tunnel结果一致,这与各组治疗机制不同有关<sup>[13-15]</sup>。刺激机体的免疫发挥抑瘤的后遗效应,是微创治疗的另一重要抗肿瘤机制。TNF-α和HSP70在肿瘤免疫中发挥重要作用,能诱导和增强机体抗肿瘤免疫反应,抑制肿瘤生长<sup>[18-19]</sup>。本实验结果显示,纳米刀治疗后可激发机体自身免疫系统,发挥抗肿瘤的后遗效应,这与纳米刀消融迅速、完全彻底、大量释放肿瘤抗原碎片、激发机体免疫系统有关。肿瘤的重要特征之一是不同阶段发生侵袭转移,VEGF是其中重要的启动子之一,肿瘤血管生成的程度间接反映了肿瘤的浸润、复发及转移的能力<sup>[20]</sup>。本研究各治疗组血浆VEGF因子水平较对照组升高,可能与肿瘤血管破坏后短时间内VEGF释放入血有关,术区VEGF表达有所下降尤以冷冻治疗组为著,这与冷冻消融的“冷冻栓塞”有关<sup>[21]</sup>,表明各治疗组能一定程度抑制血管形成因子的表达,减少肿瘤组织的血液供应,抑制癌细胞的迁移,可能是消融技术治疗肿瘤的一项重要机制。

在安全性方面,血清检测结果显示,与对照组相比,纳米刀组肌酸激酶水平升高,这可能与实验免治疗过程中的肌肉抽搐有关。冷冻及射频治疗后邻近粘连的小肠明显充血水肿,而纳米刀组未见明显肠道损伤,充分说明纳米刀消融区的边界清晰。因此,与冷冻及射频治疗相比,纳米刀更适合进展期胰腺

癌的局部减瘤治疗,尤其是包绕血管、胆管及神经等重要结构时,能有效地保存重要结构,预防严重并发症的发生<sup>[22]</sup>。

本组实验中,纳米刀治疗组在激发机体免疫和保护周围重要脏器方面有一定的优势。但是由于本研究实验样本数较少,纳米刀对比于冷冻及射频消融在胰腺癌中的应用优势、治疗各项参数的优化及选择还需更多临床前研究。

## [参考文献]

- [1] Siegel R L, Miller K D, Jemal A. Cancer statistics, 2015[J]. CA Cancer J Clin, 2015, 65:5-29.
- [2] Cunningham D, Chau I, Stocken D D, Valle J W, Smith D, Steward W, et al. Phase III randomized comparison of gemcitabine versus gemcitabine plus capecitabine in patients with advanced pancreatic cancer [J]. J Clin Oncol, 2009, 27:5513-5518.
- [3] Conroy T, Desseigne F, Ychou M, Bouché O, Guimbaud R, Bécouarn Y, et al. Groupe Tumeurs Digestives of Unicancer; PRODIGE Intergroup. FOLFIRINOX versus gemcitabine for metastatic pancreatic cancer[J]. N Engl J Med, 2011, 364: 1817-1825.
- [4] Yardley D A, Brufsky A, Coleman R E, Conte P F, Cortes J, Glück S, et al. Phase II/III weekly nab-paclitaxel plus gemcitabine or carboplatin versus gemcitabine/carboplatin as first-line treatment of patients with metastatic triple-negative breast cancer (the tnAcity study): study protocol for a randomized controlled trial[J]. Trials, 2015, 16:575.
- [5] Niu L, He L, Zhou L, Mu F, Wu B, Li H, et al. Percutaneous ultrasonography and computed tomography guided pancreatic cryoablation: feasibility and safety assessment[J]. Cryobiology, 2012, 65: 301-307.
- [6] Fegrachi S, Besselink M G, van Santvoort H C, van Hillegersberg R, Molenaar I Q. Radiofrequency ablation for unresectable locally advanced pancreatic cancer: a systematic review[J]. HPB (Oxford), 2014, 16: 119-123.
- [7] Girelli R, Frigerio I, Giardino A, Regi P, Gobbo S, Malleo G, et al. Results of 100 pancreatic radiofrequency ablations in the context of a multimodal strategy for stage III ductal adenocarcinoma [J].

- Langenbecks Arch Surg, 2013, 398:63-69.
- [8] Rubinsky B, Onik G, Mikus P. Irreversible electroporation: a new ablation modality-clinical implications[J]. Technol Cancer Res Treat, 2007, 6:37-48.
- [9] Au J T, Kingham T P, Jun K, Haddad D, Gholami S, Mojica K, et al. Irreversible electroporation ablation of the liver can be detected with ultrasound B-mode and elastography[J]. Surgery, 2013, 153:787-793.
- [10] Kingham T P, Karkar A M, D'Angelica M I, Allen P J, Dematteo R P, Getrajdman G I, et al. Ablation of perivascular hepatic malignant tumors with irreversible electroporation[J]. J Am Coll Surg, 2012, 215:379-387.
- [11] Yu Z, Zhang X, Ren P, Zhang M, Qian J. Therapeutic potential of irreversible electroporation in sarcoma[J]. Expert Rev Anticancer Ther, 2012, 12:177-184.
- [12] Lee E W, Chen C, Prieto V E, Dry S M, Loh C T, Kee S T. Advanced hepatic ablation technique for creating complete cell death: irreversible electroporation[J]. Radiology, 2010, 255:426-433.
- [13] Weaver J C. Electroporation: a dramatic, non-thermal electric field phenomenon[C]//Proceeding of the First World Congress for Electricity and Magnetism in Biology and Medicine. Lake Buena Vista. Florida: Academic Press, 1992:14.
- [14] 徐克成,牛立志.肿瘤冷冻治疗学[M].上海:上海科技教育出版社,2007: 218-225.
- [15] Fegrachi S, Molenaar I Q, Klaessens J H, Besselink M G, Offerhaus J A, van Hillegersberg R. Radiofrequency ablation of the pancreas with and without intraluminal duodenal cooling in a porcine model[J]. J Surg Res, 2013, 184:867-872.
- [16] 邵佳亮,胡国信,郑洁,万赞燕,姜瑞娇.羟基喜树碱对肝纤维化大鼠肝组织Bax、Bcl-2基因和 $\alpha$ -SMA蛋白表达及肝纤维化的影响[J].第二军医大学学报,2014, 35: 399-405.
- SHAO J L, HU G X, ZHENG J, WAN Z Y, JIANG R J. Effects of hydroxycamptothecin on hepatic expression of Bax and Bcl-2 genes and  $\alpha$ -SMA protein and hepatic fibrosis in rats[J]. Acad J Sec Mil Med Univ, 2014, 35:399-405.
- [17] 赵瑞,唐春花,赵文元,刘建民,洪波,许奕,等. Caspase-3 体外对 PIAS1 蛋白酶切作用的初步验证[J]. 第二军医大学学报,2011, 32: 1144-1146.
- ZHAO R, TANG C H, ZHAO W Y, LIU J M, HONG B, XU Y, et al. Cleavage effect of Caspase-3 on PIAS1 protein *in vitro*[J]. Acad J Sec Mil Med Univ, 2011, 32:1144-1146.
- [18] 付清松,夏玉军,张明,刘明,单守勤.三维球体间充质干细胞移植对大鼠缺血再灌注损伤脑组织TNF- $\alpha$  及凋亡相关蛋白表达的影响[J]. 第二军医大学学报, 2015, 36: 845-850.
- FU Q S, XIA Y J, ZHANG M, LIU M, SHAN S Q. Transplantation with three-dimensional spheroid-cultured mesenchymal stem cells down-regulates expression of TNF- $\alpha$  and apoptosis-related proteins in rats with cerebral ischemia/reperfusion injury [J]. Acad J Sec Mil Med Univ, 2015, 36:845-850.
- [19] Tsan M F, Gao B. Heat shock proteins and immune system[J]. J Leukoc Biol, 2009, 85:905-910.
- [20] Das M, Wakelee H. Targeting VEGF in lung cancer [J]. Expert Opin Ther Targets, 2012, 16:395-406.
- [21] Zhen W, Gang Z, Tao W, Qian F Y, Min Y S, Xiao M H. Three-dimensional numerical simulation of the effects of fractal vascular trees on tissue temperature and intracellular ice formation during combined cancer therapy of cryosurgery and hyperthermia[J]. Applied Thermal Engineering, 2015, 90: 296-304.
- [22] Hildebrand P, Leibecke T, Kleemann M, Mirow L, Birth M, Bruch H P, et al. Influence of operator experience in radiofrequency ablation of malignant liver tumours on treatment outcome[J]. Eur J Surg Oncol, 2006, 32:430-434.

〔本文编辑〕 魏学丽